

Back-in-Time Diffusion: Unsupervised Detection of Medical Deepfakes

FRED GRABOVSKI, LIOR YASUR, GUY AMIT, YUVAL ELOVICI, and YISROEL MIRSKY*, Ben-Gurion University, Israel

Recent progress in generative models has made it easier for a wide audience to edit and create image content, raising concerns about the proliferation of deepfakes, especially in healthcare. Despite the availability of numerous techniques for detecting manipulated images captured by conventional cameras, their applicability to medical images is limited. This limitation stems from the distinctive forensic characteristics of medical images, a result of their imaging process.

In this work we propose a novel anomaly detector for medical imagery based on diffusion models. Normally, diffusion models are used to generate images. However, we show how a similar process can be used to detect synthetic content by making a model reverse the diffusion on a suspected image. We evaluate our method on the task of detecting fake tumors injected and removed from CT and MRI scans. Our method significantly outperforms other state of the art unsupervised detectors with an increased AUC of 0.9 from 0.79 for injection and of 0.96 from 0.91 for removal on average.

CCS Concepts: • **Security and privacy**; • **Computing methodologies** → **Machine learning**.

Additional Key Words and Phrases: Medical Deepfake Detection, Healthcare Security, Unsupervised Learning, Anomaly Detection, Diffusion Models

1 INTRODUCTION

In recent years, the field of generative AI has gained increasing popularity with the introduction of Generative Adversarial Networks (GANs) and diffusion models which are capable of generating and editing images with impressive quality. However, these models can be used maliciously to create ‘deepfakes’; believable media created by deep neural network [28]. Deepfakes can be used to spread misinformation [1, 20], manipulate forensic evidence [23], perform blackmail [21] and even perform scams [12].

The proliferation of deepfakes can be attributed in-part to the growing accessibility of these technologies. Given the tools and online resources today, very little technical expertise is required to create a convincing deepfakes. For example, with publicly available text-to-image models [9, 31], such as Stable Diffusion [32], anyone can easily create and edit image content using only textual instructions.

The threat of deepfakes also applies to the healthcare sector. In a paper called CT-GAN [29] the authors demonstrated that malicious actors can gain access to records at a hospital and manipulate CT scans of patients with deepfake content. There are several reasons an adversary would want to perform a deepfake attack on medical imagery. For example, an attacker can add a small a brain aneurysm to his/her own MRI scan as irrefutable evidence for losing the ability to taste, enabling the attacker to collect money from a quality of life insurance policy. Moreover, an attacker can alter a medical record to cause physical or mental harm to an individual. More examples can be found in [29].

The threat of medical deepfakes is a notable concern. Numerous research papers and security reports have demonstrated that attackers can access and modify medical scans though cyber attack and physical intrusion [3, 11, 39]. Moreover, advances in generative AI enables adversaries to alter

*Corresponding author

Authors' address: Fred Grabovski, freddie@post.bgu.ac.il; Lior Yasur, lioryasu@post.bgu.ac.il; Guy Amit, guy5@post.bgu.ac.il; Yuval Elovici, elovici@bgu.ac.il; Yisroel Mirsky, yisroel@bgu.ac.il, Ben-Gurion University, 1 Ben-Gurion Ave., Beersheba, Israel.

medical evidence in a medical scan. For example, it can be used to hide the presence of a cancerous tumor to the degree of realism where both experienced radiologist and AI-tools can be deceived [29]. Moreover, with advances in text-to-image models such as [32, 34], adversaries can now tune text-to-image model using just few images instead of training it from scratch; making the threat of medical deepfakes much more viable.

A challenge with existing tamper detection models is that they are designed with the assumption that the images were captured using a conventional camera. Conventional cameras use CMOS (Complementary Metal-Oxide Semiconductor) or CCD (Charge-Coupled Device) imaging sensors which *linearly* maps received light to pixels in an image. This results in uniform noise patterns in the image which can be utilized to detect image tampering [24]. However, medical imaging devices capture images in a very different manner resulting in non-uniform forensic patterns. For example, CT scanner uses X-rays to capture multiple cross-sectional views of an object from different angles. These views are then processed using a radon transform to reconstruct the internal image (slice). As a result, many existing detection methods, such as [5–7, 13], cannot detect medical deepfakes very well (demonstrated in section 5).

In this paper, we introduce a deepfake image detector for medical images. Our detector uses a technique we call Back-in-Time Diffusion (BTD) which utilizes the generative abilities of Denoising Diffusion Probabilistic Models (DDPMs) to reveal synthetic forensics as residuals. We found that a single step of the backward diffusion denoising process removes synthetic forensic patterns left by other models. As a result, we can produce an anomaly score by measuring the residual between the backwards-diffused image and the original image.

The proposed DDPM model is trained in an unsupervised manner on the target domain (e.g., random CT scans of the same organs), meaning that there is no need for data labeling. This makes the model practical to train and enables the model to generalize to unseen deepfake technologies. We evaluate BTD on deepfake-tampered CT and MRI medical scans and show that BTD outperforms other state-of-the-art detectors with an AUC of 0.9 compared to 0.79 for detecting injection deepfakes and an AUC of 0.96 compared to 0.91 for removal on average. To test our method, we have created six novel datasets containing deepfake medical images, using CT-GAN and modern generative models such as Stable Diffusion.

In summary our contributions are:

- A novel technique for detecting forensic anomalies in images, evaluated on various medical imaging modalities. The method outperforms other state-of-the-art techniques at detecting medical deepfakes.
- We have created and published six new medical deepfake evaluation datasets using state of the art techniques which the community can use as benchmarks.

2 RELATED WORK

The exploration of tamper detection in images has evolved significantly, initially centering on conventional manipulation techniques like splicing and copy-move [6, 26, 37]. However, the advent of advanced generative models such as GANs and diffusion models has shifted focus towards detecting images synthesized through deep learning [8, 14, 18].

Supervised approaches to deepfake detection necessitate extensive training datasets that cover all types of deepfakes [38, 41]. This is particularly challenging due to the rapid evolution of deepfake technology and the scarcity of comprehensive datasets, especially in the medical domain.

To counter this challenge, unsupervised learning techniques can be used. Two prevalent methods for detecting image anomalies in an unsupervised setting are: reconstruction-based approaches and fingerprint-based approaches.

Reconstruction-based approaches rely on modeling genuine image distributions and then identifying samples that deviate from them. For example an autoencoder (AE) or Vision Transformer (ViT) can be used to detect manipulated images by identifying cases where the model fails to reconstruct the same image (indicating an outlier) [10, 33, 43]. Such methods compress and reconstruct the entire image, potentially smoothing over subtle distortions, unlike BTD which effectively captures these distortions by strategically applying only a small number of backward steps in the diffusion process. This approach meticulously peels back the layers of noise added during image manipulation, revealing underlying discrepancies. Using this method, BTD exposes potential tampering, making it adept at identifying manipulations that other methods might miss due to their broader reconstruction approach.

Other methods using diffusion models have also been adapted to the task of anomaly detection. For example, the authors of [15, 16, 25] utilize these models by performing forward diffusion and backward diffusion, and then by comparing the source image to the reconstructed image. In contrast, BTD only utilizes the backward diffusion for a small number of steps, resulting in faster inference. Furthermore, we found that these methods result in poor tamper detection performance because they add high levels of noise which obscures the subtle forensic evidence around the tampered areas (see section 5). Additionally, some works suggest using conditional diffusion models for specific anomaly detection tasks [30, 40]. However, compared to BTD, these approaches are supervised, making them impractical for detecting medical deepfakes. This is because it would require curating and maintaining an up to date large scale medical deepfake dataset.

Fingerprint-based methods are a popular choice in tampering detection. They model the imaging process, specifically the noise infused to the image [4, 5, 27]. Such modeling usually relies on the assumption that images from different imaging devices contain different noise imaging patterns (noise fingerprint) [4, 7, 13]. Under this assumption, image parts identified with a different imaging device than the original device are considered to be modified by a third-party.

The idea of image consistency, i.e. that all image parts must share the same noise fingerprint, was extended to other properties of the image. For example, the ComPrint method [27] checks the consistency of compression types (JPEG, PNG...) among image patches. In general, images are characterized by various properties that are stored in the image metadata (EXIF), which can be checked for consistency as well [20]. Unfortunately, the metadata required for implementing these methods is not available in medical imaging databases. For instance, medical images are not compressed, and medical datasets usually contain data from only a few types of imaging devices (scanners). Therefore, their application to medical imagery is limited.

Furthermore, it is important to note that the imaging processes in medical devices (such as MRI and CT) is different than in standard cameras. In particular, medical devices model the difference in radiation between a transmitter and a detector, whereas standard cameras capture the incoming light using a spatial array of sensors. Consequently, methods built on assumptions related to the camera’s hardware may need adjustments in order to be successfully applied to medical scans, and therefore perform sub-optimally on medical imagery.

In contrast, our Back-in-Time Diffusion (BTD) technique leverages the unsupervised potential of Denoising Diffusion Probabilistic Models (DDPMs) to offer a versatile solution for detecting manipulated images, bypassing the limitations of existing methods in the medical domain and in additional scenarios in which the imaging process is different or the availability of image meta data is limited.

3 BACK-IN-TIME DIFFUSION

Denoising diffusion probabilistic models (DDPM) [18] are a class of generative models which are inspired by concepts from nonequilibrium thermodynamics.

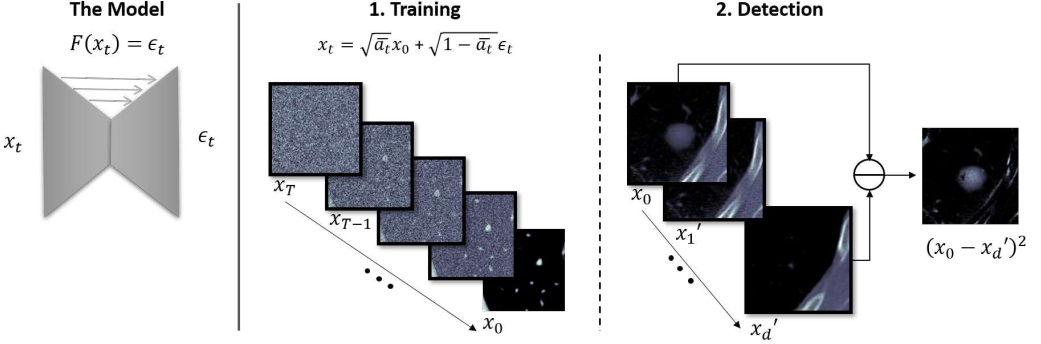


Fig. 1. Overview of the Back-in-Time Diffusion framework. The model is a U-net that predicts the noise added in the last step ($F(x_t) \Rightarrow \epsilon_t$). The train set is created by taking images (x_0) and noising them to some x_t . Detection is performed on image x_0 by measuring the error after d steps.

DDPMs utilize two processes (1) forward diffusion, which is the process of noising an input sample $x_0 \sim q(x_0)$ into a noise $x_T \sim \mathcal{N}(0, I)$, and (2) the backward diffusion process, that reverses the forward diffusion process, from x_T to x_0 using T time steps.

The training of DDPMs is an iterative process, where in each iteration, a random number of steps t is selected, and the forward diffusion process is used to noise an input sample x_0 into x_t over t steps using a closed mathematical formula

$$x_t = \sqrt{\alpha_t} \cdot x_0 + \sqrt{1 - \alpha_t} \cdot \epsilon_t \quad (1)$$

where $\epsilon_t \sim \mathcal{N}(0, I)$ and $\alpha_t = \prod_{i=1}^t \alpha_i$ is a term responsible for controlling the image content loss in each time step of the forward process. After the noised sample x_t is calculated, the backward diffusion process uses a U-Net-like [36] neural network $\epsilon_\theta(\cdot, \cdot)$ to estimate the noise ϵ_t from x_t . The neural network is then updated according to a gradient step minimizing the squared difference between the noise ϵ_t and the neural network output $\epsilon_\theta(x_t, t)$:

$$loss = \|\epsilon_t - \epsilon_\theta(x_t, t)\|^2 \quad (2)$$

Finally, after the neural network's training has converged, the backward diffusion process can be used to sample new images. The process starts from noise $\epsilon \sim \mathcal{N}(0, I)$ and then repeatedly estimates x_{t-1} from x_t , until $t = 0$, resulting in a sample x_0 similar to samples in the training set. More details about diffusion models can be found at [9, 18].

As discussed in Section 3, the backward diffusion process used in DDPMs gradually converts Gaussian noise to an image x_0 from the training distribution. In BTD, we utilize the backward diffusion process as a mechanism for detecting fake image content.

BTD Diffusion Step. After a DDPM has been trained, the resulting model is usually used to produce x_{t-1} from x_t ; typically, this process repeats until $t = 0$. However, We have found that starting the process from a source image x_0 and running it for d steps, will result in an image x_d' that reconstructs parts of the original image. This process is visually illustrated in Figure 1. In practice, we have found that limiting the backward diffusion process to a small number of steps, specifically to $d = 1$, yields the best performance. This is because fewer denoising iterations minimize alterations to the genuine content while still modifying the subtle patterns and cues that differentiate real from fake images. Multiple iterations, however, tend to over-normalize both real and manipulated areas, diminishing the distinctive features crucial for accurate anomaly detection.

BTD Detection Step. If the model has been trained on benign imagery only (i.e., real medical scans), then the diffusion process will fail to maintain any synthetic (deepfake) content during the diffusion process. To detect this content we calculate the Mean Squared Error (MSE) of the residual (between x_0 and x_d). This anomaly score is computed as:

$$\frac{1}{W \times H} \sum_{i=1}^{W \times H} (x_0(i) - x'_d(i))^2$$

where W and H are the width and height of the image respectively. The larger the score, the more likely x_0 is anomalous. In the case of injection, we improve the results by taking the average over the center of $(x_0(i) - x'_d(i))^2$ (e.g. a 32x32 patch). The identification of fake samples is performed by flagging samples corresponding to an anomaly score greater than some predetermined threshold τ . the prediction is performed using the following formula:

$$p(score) = \begin{cases} R & \text{if } \tau \leq score \\ F & \text{if } \tau > score \end{cases} \quad (3)$$

where R stands for real images, and F stands for deepfake images. The threshold can be determined statistically by analyzing the scores of normal data and setting τ to be high enough such that normal data will likely produce scores less than τ .

Detection Stability. DDPMs are known for their stochastic nature, attributed to the random noise sampled during the backward diffusion process. Deploying a DDPM based detection tool may raise some understandable concerns regarding the stability and reproducibility of detection performance. However, in our experiments we have found that using a small number of backward diffusion steps, specifically $d = 1$, results in a negligible variance in reconstruction, effectively eliminating stochastic variability in the outputs and ensuring consistent performance.

4 EXPERIMENTAL SETUP

In this section, we evaluate BTD’s ability to detect deepfakes in CT lung and MRI breast scans. We consider two different attack scenarios: injection and removal of tumors. In the case of injection, samples representing authentic images with malignant tumors are called True-Malign (TM) samples, and those with artificially inserted malignant tumors are called Fake-Malign (FM) samples. Similarly, for removal, True-Benign (TB) samples are genuine benign images and Fake-Benign (FB) samples are images with artificially removed tumors. Authentic TM and TB images were sourced from the Duke Breast Cancer MRI dataset [35] and the LIDC dataset [2]. To create FM and FB images, we utilized the CT-GAN [29] for targeted tumor manipulation in CT scans and fine-tuned Stable Diffusion models [32, 34] (denoted as SD) for both CT and MRI image manipulations.

We compiled six datasets for evaluation: CTGAN-CT-Inject, CTGAN-CT-Remove, SD-CT-Inject, SD-CT-Remove, SD-MRI-Inject, and SD-MRI-Remove. These datasets consist of five different scanners for CT and four different scanners for MRI. Sample images from our datasets are provided in Figure 2 where we show the before and after of applying the attacks.

Datasets were divided into training, validation, and testing sets, ensuring no patient overlap to avoid bias. The training set consisted solely of true images (TM, TB), with around 77,000 CT slices and 47,000 MRI slices. Similarly, the validation set also included only true images, comprising approximately 17,000 CT slices and 14,000 MRI slices. As part of the data preparation, MRI slices were standardized on a per-patient basis, whereas CT image values were clipped at -700 (Air) and 2000 (Bone) thresholds. Both image modalities were then scaled to a [0, 1] range.

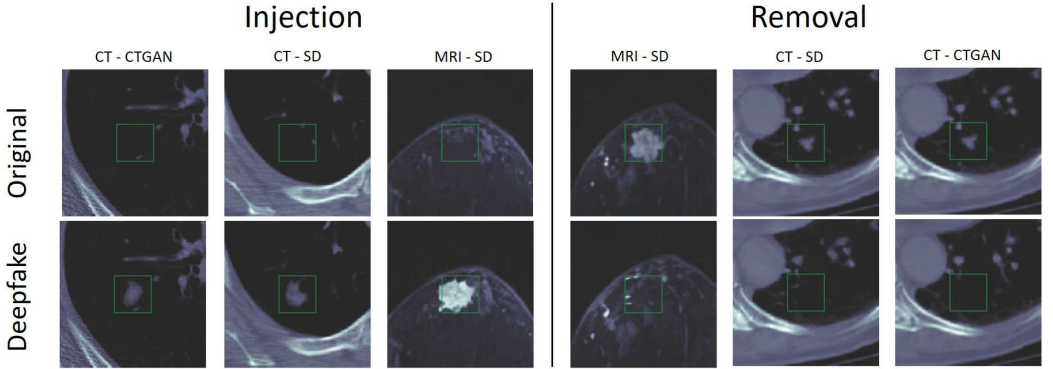


Fig. 2. Examples of manipulated images from our detection datasets. Top: original images. Bottom: images after being edited by generative models

To apply BTD, we first extract a patch around the area of interest and then pass it through our model. We set the patch sizes to 96x96 and 128x128 for CT and MRI respectively to encapsulate potential tumors with sufficient context.

BTD Hyperparameters and Hardware Setup. Our framework revolves around a UNET-based Diffusion model, for which we used the default hyper-parameters as outlined in ¹, with the exception of the model’s dimensions and batch size, which we changed to 32 init_features and 64 respectively.

The training of all the models used for this paper evaluation was performed using RTX 4090 NVIDIA GPUs.

Baselines. To ensure a fair comparison, we focused on unsupervised image anomaly detection models that do not rely on additional metadata, such as DICOM tags. To represent the popular AE techniques, we used as basic AE, U-net, in-painting AE, and an OC-VAE [17, 22, 33, 42, 43]. To consider the image forensics domain, we used SpliceBuster [6] and SpliceRadar [13]. SpliceBuster employs a Gaussian Mixture Model and noise extraction to segment images into regions suspected as real and counterfeit. SpliceRadar employs a deep neural network for advanced image forensics. Finally, to represent modern methods, we use the vision transformer Satellite ViT [10, 19] and an Out-of-distribution (OOD) detection method based on DDPMs [16]. Whenever possible, we utilized the authors’ code.

Metrics. Performance was measured using area under the curve (AUC) and equal error rate (EER). A higher AUC and lower EER indicate better performance. Our evaluation metrics are calculated using bootstrap sampling with 100 iterations, where in each iteration the number of samples per class were balanced across the scanners in the dataset. The results presented in the paper are the means calculated across the 100 iterations.

5 RESULTS

In this section, we evaluate the capability of BTD in detecting deepfake medical images. We start by comparing BTD’s performance to competing methods in the field, followed by an analysis of how different factors affect BTD’s performance.

Table 1. Baselines comparison: AUC and EER results. Bold results are the best and underlined are the second best. CT-GAN is annotated as CT-G

	AUC \uparrow						EER \downarrow						
	Injection			Removal				Injection			Removal		
	MRI	CT	SD	MRI	CT	SD		MRI	CT	SD	MRI	CT	SD
	SD	CT-G	SD	SD	CT-G	SD		SD	CT-G	SD	SD	CT-G	SD
AE	0.80	0.56	0.79	0.91	0.45	<u>0.93</u>	0.25	0.46	0.28	0.17	0.54	0.11	
In-Paint AE	0.52	<u>0.80</u>	0.76	0.65	0.60	0.56	0.48	0.25	0.31	0.39	<u>0.44</u>	0.48	
OC-VAE	0.54	0.62	0.68	0.58	0.48	0.52	0.48	0.40	0.38	0.48	0.51	0.49	
Unet-AE	0.63	0.46	0.71	0.73	0.48	0.92	0.43	0.51	0.47	0.34	0.50	0.43	
Splice Buster	0.48	0.49	0.54	0.46	0.50	0.59	0.50	0.51	0.47	0.49	0.52	0.45	
Splice Radar	0.55	0.73	0.61	0.62	<u>0.57</u>	0.65	0.47	0.34	0.41	0.44	0.44	0.40	
Satellite ViT	0.54	0.61	0.65	0.63	0.47	0.51	0.42	0.42	0.39	0.42	0.50	0.48	
OOD DDPM	0.50	0.54	0.53	0.63	0.42	0.49	0.48	0.45	0.46	0.43	0.57	0.52	
BTD - 32 dim	0.99	0.81	0.91	0.98	0.55	0.86	0.08	<u>0.28</u>	0.18	0.08	0.46	0.22	
BTD - 8 dim	<u>0.93</u>	0.69	<u>0.87</u>	<u>0.93</u>	0.52	0.94	<u>0.14</u>	0.38	<u>0.21</u>	<u>0.12</u>	0.48	<u>0.13</u>	

5.1 Baseline Analysis

In Table 1 we present the detection performance of two BTD detectors using different parameters (`init_features` of 8 and 32). The table shows that BTD outperforms the other baselines with a significant margin. This is regardless of whether the baseline was designed to detect semantic anomalies (e.g., the AE variants) or forensic anomalies (Splice detectors and Satellite ViT). The exception to this observation is on the dataset (CTGAN-CT-Remove) where *all* of the methods fail, including BTD. For this dataset, every method obtains an AUC of about 0.55 where In-Paint AE received the highest performance of 60. We believe that the reason for this is that there are very few semantic anomalies left behind after a removal attack. Therefore, the models must rely on forensic anomalies alone to identify tampering (e.g., noise patterns). However, in this dataset, CT-GAN uses noise to further mask the removal of tumors. This is why all of the methods struggle to identify the attack.

In summary, BTD performs very well at detecting medical deepfakes across different modalities, such as CT and MRI scans. Similar to existing detection algorithms, BTD relies on the availability of forensic or semantic evidence to operate effectively. The issue of obscured forensics is an open research problem which we leave to future work.

5.2 BTD’s Ablation Study

In this section, we analyze how the number of backward diffusion steps and the tumor size affect BTD’s detection performance.

Number of Diffusion steps. The hyper-parameter d is the number of backward diffusion steps performed by BTD. In Figure 3 we plot its impact on detection performance for each of the datasets. Our first observation is that, with enough iterations, the injection-detection performance begins to increase and then plateaus around $d \approx 400$. We believe this is because the BTD denoising steps gradually remove the forensic patterns making it easier to contrast the fake content. Our second observation was that more than one iteration on MRI scans significantly harms the detection of injected tumors. This might be due to the fact that MRI scans of breast tissue are densely packed with textures and patterns whereas CT images in our datasets are sparse and less complex. As the

¹<https://github.com/lucidrains/denoising-diffusion-pytorch>

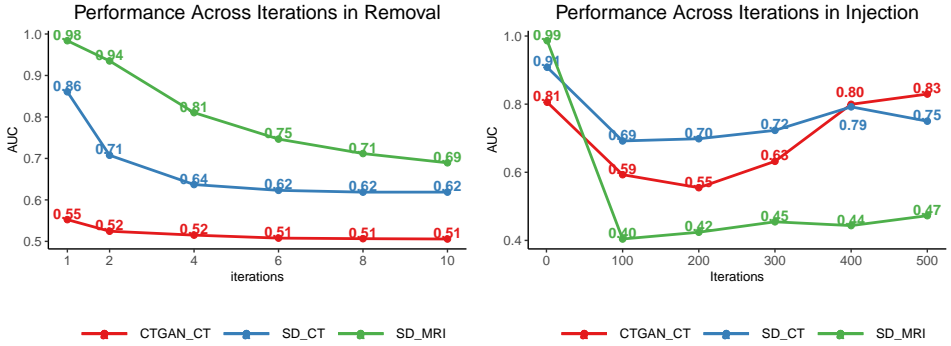


Fig. 3. The impact of diffusion step count on BTD performance for removal (left) and injection (right).

Tumor Size Analysis

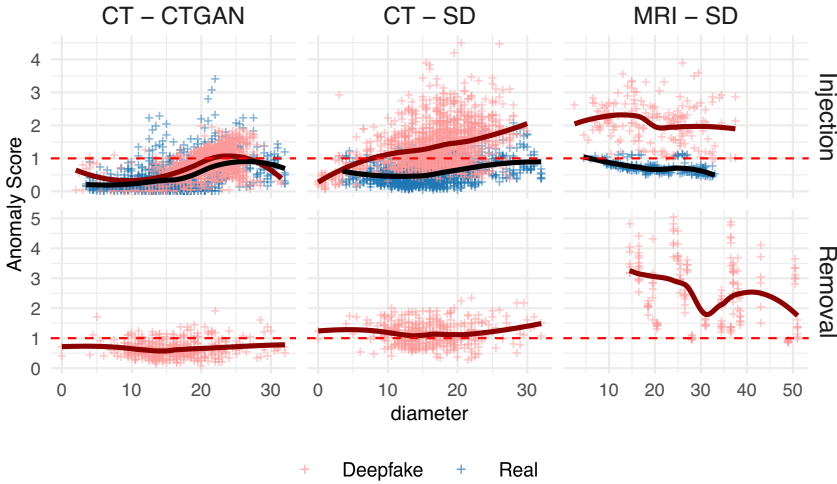


Fig. 4. The impact tumor size has on BTD detection performance. Anomaly scores are normalized to a false positive rate (FPR) of 0.1 (values over the red dashed line are anomalies). In datasets of removal (bottom row), real images (TB) are omitted as they lack tumors.

backward diffusion process removes the tumor, it degrades more spatial information in the MRI images than in the CT images, causing a significant drop in the model's ability to detect semantic anomalies.

In general, we found that fewer diffusion steps ($d \approx 1$) is preferred for detecting removal and injection attacks in all cases.

Tumor size. It might be assumed that larger tampered areas would be easier to detect given the presence of more evidence. While this phenomenon exists in the CT injection datasets, in Figure 4 we show that the opposite is true for the MRI datasets. Upon further investigation, we found that SD tends to modify more of the image when the mask of the tumor is larger. This means that when larger masks are used, BTD has less contextual information to use to detect semantic anomalies.

This is why larger tumors are slightly harder to detect than smaller ones for MRI compared to CT where the mask size is constant. In CT removal scenarios there is no correlation to tumor size because CTGAN always tampers the same sized area of 32x32x32, regardless of how large the tumor was. Similarly, Uniform mask sizes of 32x32 were used to remove tumors in CT with Stable Diffusion as well. Despite these observations, we see that fake tumors have consistently higher BTD-anomaly scores, regardless of their size.

6 CONCLUSION

In this paper, we presented Back-in-Time Diffusion (BTD), a novel approach for identifying medical deepfakes. BTD surpasses current methodologies, establishing a new benchmark for detecting tampered medical images. It exhibits robustness across a diverse set of medical imaging modalities (CT and MRI) and deepfake attacks (injection and removal). Moreover, the method's efficacy against different deepfake generation technologies (CT-GAN and SD) further underscores its adaptability and robustness. However, despite these achievements, challenges in deepfake detection still persist. For instance, BTD, along with all other methods, struggles to detect tumors that have been removed from CT images using CT-GAN. Finally, as future work, it would be interesting to explore the application of BTD to other domains, such as classical image forensics.

REFERENCES

- [1] Zahid Akhtar. 2023. Deepfakes Generation and Detection: A Short Survey. *Journal of Imaging* 9, 1 (2023), 18.
- [2] SG Armato III, G McLennan, L Bidaut, MF McNitt-Gray, CR Meyer, AP Reeves, B Zhao, DR Aberle, CI Henschke, EA Hoffman, et al. 2015. Data from LIDC-IDRI [data set]. *The Cancer Imaging Archive* 10 (2015), K9.
- [3] Christiaan Beek. 2018. McAfee researchers find poor security exposes medical data to cybercriminals. *McAfee Blogs* (2018).
- [4] Mo Chen, Jessica Fridrich, Miroslav Goljan, and Jan Lukás. 2008. Determining image origin and integrity using sensor noise. *IEEE Transactions on information forensics and security* 3, 1 (2008), 74–90.
- [5] Davide Cozzolino, Francesco Marra, Giovanni Poggi, Carlo Sansone, and Luisa Verdoliva. 2017. PRNU-based forgery localization in a blind scenario. In *Image Analysis and Processing-ICIAP 2017: 19th International Conference, Catania, Italy, September 11-15, 2017, Proceedings, Part II* 19. Springer, 569–579.
- [6] Davide Cozzolino, Giovanni Poggi, and Luisa Verdoliva. 2015. Splicebuster: A new blind image splicing detector. In *2015 IEEE International Workshop on Information Forensics and Security (WIFS)*. IEEE, 1–6.
- [7] Davide Cozzolino and Luisa Verdoliva. 2019. Noiseprint: A CNN-based camera model fingerprint. *IEEE Transactions on Information Forensics and Security* 15 (2019), 144–159.
- [8] Antonia Creswell, Tom White, Vincent Dumoulin, Kai Arulkumaran, Biswa Sengupta, and Anil A Bharath. 2018. Generative adversarial networks: An overview. *IEEE signal processing magazine* 35, 1 (2018), 53–65.
- [9] Florinel-Alin Croitoru, Vlad Hondu, Radu Tudor Ionescu, and Mubarak Shah. 2023. Diffusion models in vision: A survey. *IEEE Transactions on Pattern Analysis and Machine Intelligence* (2023).
- [10] Alexey Dosovitskiy, Lucas Beyer, Alexander Kolesnikov, Dirk Weissenborn, Xiaohua Zhai, Thomas Unterthiner, Mostafa Dehghani, Matthias Minderer, Georg Heigold, Sylvain Gelly, et al. 2020. An image is worth 16x16 words: Transformers for image recognition at scale. *arXiv preprint arXiv:2010.11929* (2020).
- [11] Marco Eichelberg, Klaus Kleber, and Marc Kämmerer. 2020. Cybersecurity in PACS and medical imaging: an overview. *Journal of Digital Imaging* 33, 6 (2020), 1527–1542.
- [12] Guy Frankovits and Yisroel Mirsky. 2023. Discussion Paper: The Threat of Real Time Deepfakes. *arXiv preprint arXiv:2306.02487* (2023).
- [13] Aurobrata Ghosh, Zheng Zhong, Terrance E Boult, and Maneesh Singh. 2019. SpliceRadar: A Learned Method For Blind Image Forensics.. In *CVPR Workshops*. 72–79.
- [14] Ian Goodfellow, Jean Pouget-Abadie, Mehdi Mirza, Bing Xu, David Warde-Farley, Sherjil Ozair, Aaron Courville, and Yoshua Bengio. 2020. Generative adversarial networks. *Commun. ACM* 63, 11 (2020), 139–144.
- [15] Joseph Goodier and Neill DF Campbell. 2023. Likelihood-based Out-of-Distribution Detection with Denoising Diffusion Probabilistic Models. *arXiv preprint arXiv:2310.17432* (2023).
- [16] Mark S Graham, Walter HL Pinaya, Petru-Daniel Tudosiu, Parashkev Nachev, Sébastien Ourselin, and Jorge Cardoso. 2023. Denoising diffusion models for out-of-distribution detection. In *Proceedings of the IEEE/CVF Conference on Computer Vision and Pattern Recognition*. 2947–2956.

- [17] Matthias Haselmann, Dieter P Gruber, and Paul Tabatabai. 2018. Anomaly detection using deep learning based image completion. In *2018 17th IEEE international conference on machine learning and applications (ICMLA)*. IEEE, 1237–1242.
- [18] Jonathan Ho, Ajay Jain, and Pieter Abbeel. 2020. Denoising diffusion probabilistic models. *Advances in neural information processing systems* 33 (2020), 6840–6851.
- [19] János Horváth, Sriram Baireddy, Hanxiang Hao, Daniel Mas Montserrat, and Edward J Delp. 2021. Manipulation detection in satellite images using vision transformer. In *Proceedings of the IEEE/CVF Conference on Computer Vision and Pattern Recognition*. 1032–1041.
- [20] Minyoung Huh, Andrew Liu, Andrew Owens, and Alexei A Efros. 2018. Fighting fake news: Image splice detection via learned self-consistency. In *Proceedings of the European conference on computer vision (ECCV)*. 101–117.
- [21] Byan Ke. 2022. Singaporean man's face ends up in deepfake porn after he refuses to pay hacker \$5,800. <https://news.yahoo.com/singaporean-mans-face-ends-deepfake-171743924.html>. (Accessed on 08/30/2023).
- [22] Hasam Khalid and Simon S Woo. 2020. OC-FakeDect: Classifying deepfakes using one-class variational autoencoder. In *Proceedings of the IEEE/CVF conference on computer vision and pattern recognition workshops*. 656–657.
- [23] Dahun Kim, Sanghyun Woo, Joon-Young Lee, and In So Kweon. 2019. Deep video inpainting. In *Proceedings of the IEEE/CVF Conference on Computer Vision and Pattern Recognition*. 5792–5801.
- [24] Paweł Korus and Jiwu Huang. 2016. Multi-scale analysis strategies in PRNU-based tampering localization. *IEEE Transactions on Information Forensics and Security* 12, 4 (2016), 809–824.
- [25] Victor Livernoche, Vineet Jain, Yashar Hezaveh, and Siamak Ravanbakhsh. 2023. On Diffusion Modeling for Anomaly Detection. *arXiv preprint arXiv:2305.18593* (2023).
- [26] Siwei Lyu, Xunyu Pan, and Xing Zhang. 2014. Exposing region splicing forgeries with blind local noise estimation. *International journal of computer vision* 110 (2014), 202–221.
- [27] Hannes Mareen, Dante Vanden Bussche, Fabrizio Guillaro, Davide Cozzolino, Glenn Van Wallendael, Peter Lambert, and Luisa Verdoliva. 2022. Comprint: Image forgery detection and localization using compression fingerprints. In *International Conference on Pattern Recognition*. Springer, 281–299.
- [28] Yisroel Mirsky and Wenke Lee. 2021. The creation and detection of deepfakes: A survey. *ACM Computing Surveys (CSUR)* 54, 1 (2021), 1–41.
- [29] Yisroel Mirsky, Tom Mahler, Ilan Shelef, and Yuval Elovici. 2019. {CT-GAN}: Malicious tampering of 3d medical imagery using deep learning. In *28th USENIX Security Symposium (USENIX Security 19)*. 461–478.
- [30] Arian Mousakhani, Thomas Brox, and Jawad Tayyub. 2023. Anomaly Detection with Conditioned Denoising Diffusion Models. *arXiv preprint arXiv:2305.15956* (2023).
- [31] Aditya Ramesh, Mikhail Pavlov, Gabriel Goh, Scott Gray, Chelsea Voss, Alec Radford, Mark Chen, and Ilya Sutskever. 2021. Zero-shot text-to-image generation. In *International Conference on Machine Learning*. PMLR, 8821–8831.
- [32] Robin Rombach, Andreas Blattmann, Dominik Lorenz, Patrick Esser, and Björn Ommer. 2022. High-Resolution Image Synthesis With Latent Diffusion Models. In *Proceedings of the IEEE/CVF Conference on Computer Vision and Pattern Recognition (CVPR)*. 10684–10695.
- [33] Olaf Ronneberger, Philipp Fischer, and Thomas Brox. 2015. U-net: Convolutional networks for biomedical image segmentation. In *Medical Image Computing and Computer-Assisted Intervention—MICCAI 2015: 18th International Conference, Munich, Germany, October 5–9, 2015, Proceedings, Part III* 18. Springer, 234–241.
- [34] Nataniel Ruiz, Yuanzhen Li, Varun Jampani, Yael Pritch, Michael Rubinstein, and Kfir Aberman. 2023. Dreambooth: Fine tuning text-to-image diffusion models for subject-driven generation. In *Proceedings of the IEEE/CVF Conference on Computer Vision and Pattern Recognition*. 22500–22510.
- [35] Ashirbani Saha, Michael R Harowicz, Lars J Grimm, Jingxi Weng, EH Cain, CE Kim, SV Ghate, R Walsh, and Maciej A Mazurowski. 2021. Dynamic contrast-enhanced magnetic resonance images of breast cancer patients with tumor locations [Data set]. *The Cancer Imaging Archive* (2021).
- [36] Nahian Siddique, Sidike Paheding, Colin P Elkin, and Vijay Devabhaktuni. 2021. U-net and its variants for medical image segmentation: A review of theory and applications. *Ieee Access* 9 (2021), 82031–82057.
- [37] Luisa Verdoliva. 2020. Media forensics and deepfakes: an overview. *IEEE Journal of Selected Topics in Signal Processing* 14, 5 (2020), 910–932.
- [38] Xin Wang, Hui Guo, Shu Hu, Ming-Ching Chang, and Siwei Lyu. 2022. Gan-generated faces detection: A survey and new perspectives. *arXiv preprint arXiv:2202.07145* (2022).
- [39] Zack Wittaker. 2020. A billion medical images are exposed online, as doctors ignore warnings | TechCrunch. <https://techcrunch.com/2020/01/10/medical-images-exposed-pacs/>. (Accessed on 11/06/2021).
- [40] Julia Wolleb, Florentin Bieder, Robin Sandkühler, and Philippe C Cattin. 2022. Diffusion models for medical anomaly detection. In *International Conference on Medical image computing and computer-assisted intervention*. Springer, 35–45.
- [41] Yue Wu, Wael Abd-Almageed, and Prem Natarajan. 2018. Busternet: Detecting copy-move image forgery with source/target localization. In *Proceedings of the European conference on computer vision (ECCV)*. 168–184.

- [42] Jie Yang, Ruijie Xu, Zhiqian Qi, and Yong Shi. 2021. Visual anomaly detection for images: A survey. *arXiv preprint arXiv:2109.13157* (2021).
- [43] Chong Zhou and Randy C Paffenroth. 2017. Anomaly detection with robust deep autoencoders. In *Proceedings of the 23rd ACM SIGKDD international conference on knowledge discovery and data mining*. 665–674.